

Improved basis selection for the Projected Configuration Interaction method applied to heavy nuclei

Zao-Chun Gao^{1,2}, Mihai Horoi¹, and Y. S. Chen²

¹*Department of Physics, Central Michigan University, Mount Pleasant, Michigan 48859, USA*

²*China Institute of Atomic Energy P.O. Box 275-18, Beijing 102413, China*

(Dated: November 29, 2018)

In a previous paper we proposed a Projected Configuration Interaction method that uses sets of axially deformed single particle states to build up the many body basis. We show that the choice of the basis set is essential for the efficiency of the method, and we propose a newly improved algorithm of selecting the projected basis states. We also extend our method to model spaces that can accommodate both parities, and can include odd-multipole terms in the effective interaction, such as the octupole contributions. Examples of ^{52}Fe , ^{56}Ni , ^{68}Se , ^{70}Se and ^{76}Se are calculated showing good agreement with the full Configuration Interaction results.

PACS numbers: 21.60.Cs, 21.60.Ev, 21.10.-k

I. INTRODUCTION

The full configuration interaction (CI) method [1, 2] using a spherical single particle (s.p.) basis and realistic Hamiltonians, also known as the nuclear shell model, has been very successful in describing various properties of the low-lying states in light and medium nuclei. The main limitations of this method are the exploding dimensions with the increase of the number of valence nucleons, or/and with the increase of the valence space. Although, there are continuous improvements to the CI codes [3, 4] and computational resources, the exploding CI dimensions significantly restrict the ability to investigate heavy nuclei, especially those which exhibit strong collectivity. The deformed mean-field approaches, however, have the ability to incorporate the collective effects at the single particle level. The mean-field description in the intrinsic frame naturally takes advantage of the spontaneous symmetry breaking. This approach provides some physical insight, but the loss of good angular momentum of the mean-field wave functions makes the comparison with the experimental data difficult. The CI calculations in spherical basis provide the description in the laboratory frame. The angular momentum is conserved, but the physical insight associated with the existence of an intrinsic state is lost. One important aspect of the CI approach is its ability of using all components of effective interactions compatible with a given symmetry, but restricted to a chosen valence space. Examples of realistic Hamiltonians, such as the USD [1, 5] in the sd shell, the KB3 [6], FPD6 [7] and GXPF1 [8] in the pf shell, have provided a very good base to study various nuclear structure problems microscopically.

The recent history of projection techniques combined with CI particle-hole configurations includes the Projected Shell Model (PSM) [9, 10] and the Deformed Shell Model (DSM) proposed in reference [11]. PSM uses a deformed intrinsic Nilsson+BCS basis projected onto good angular momentum, and a multipole-multipole Hamiltonian that diagonalized in the space spanned by the projected states. The Nilsson model [12] has been proven

to be very successful in describing the deformed intrinsic single particle states, and the quadrupole force was found to be essential for describing the rotational motion [13]. PSM was proven to be a very efficient method in analyzing the phenomena associated with the rotational states, especially the high spin states, not only for axial quadrupole deformation, but also for the octupole [10] and triaxial shapes [14, 15]. However, its predictive power is limited because the multipole-multipole plus pairing Hamiltonian has to be tuned to a specific class of states, rather than a region of the nuclear chart. The recently proposed DSM is using the same realistic effective Hamiltonian as the full CI method, and a Hartree-Fock procedure to select the deformed basis. One can only assume that this procedure would not be very accurate for quasi-spherical nuclei. The main difficulties for all these models is a proper selection of the deformed basis. Their accuracy can only be assessed by comparison with the exact results provided by the full CI method using the same effective Hamiltonian, and not by direct comparison with the experimental data. Other model using similar techniques includes MONSTER, the family of VAMPIRs [16], and the Quantum Monte Carlo Diagonalization (QMCD) method [17].

In a previous paper [18] we proposed a new method of calculating the low-lying states in heavy nuclei using many particle-hole configurations of spin-projected Slater determinants built on multiple sets of deformed single particle orbitals. This Projected Configuration Interaction (PCI) method takes advantage of inherent mixing induced by the projected Slater determinants of varying deformations with the many particle-hole mixing typical for the Configuration Interaction (CI) techniques. Direct comparison between PCI and CI results are always possible, provided that the deformed s.p. states are always obtained starting from a valence space of spherical orbitals. In Ref. [18] we use a simple mechanism of selecting a number of basic deformed Slater determinants in the sd and pf model space, denoted $|\kappa_j\rangle$, $0 <$, by searching for the minimum energy of fixed configuration of deformed s.p. orbitals. Starting from each basic

deformed Slater determinant, a number of particle-hole excited configurations were considered under some selection criteria (see Eq. (23) of Ref. [18]) to keep the total number of basis states manageable. Having the deformed basis of Slater determinants chosen, one can use standard spin projection techniques to solve the associated eigenvalues problem. The method proved to be very accurate in $0\hbar\omega$ model spaces, such as *sd* and *pf* where one can easily keep track of different deformed orbitals. The difficulties usually appear for quasi-spherical nuclei, such as ^{56}Ni , when special attention has to be given to the selection of the basic states $|\kappa_j, 0\rangle$. A similar problem arises for the case of mixed parity valence space, such as *f5pg9* (see below), due to difficulties in tracking fixed configurations of nucleons filling the s.p. orbitals around the level-crossing deformations.

The paper is organized as follows. Section II presents a brief outline of the PCI formalism that was expanded in Ref. [18]. The new algorithm to select the PCI basis is discussed in section III. Section IV analyzes the efficiency of the new method in the case of the quasi-spherical nucleus ^{56}Ni . Section V is devoted to the study of several nuclei that can be described using the mixed parity valence space *f5pg9*. Conclusions and outlook are given in section VI.

II. THE METHOD OF THE PROJECTED CONFIGURATION INTERACTION (PCI)

The model Hamiltonian used in CI calculations can be written as:

$$H = \sum_i e_i c_i^\dagger c_i + \sum_{i>j,k>l} V_{ijkl} c_i^\dagger c_j^\dagger c_l c_k, \quad (1)$$

where, c_i^\dagger and c_i are creation and annihilation operators of the spherical harmonic oscillator, e_i and V_{ijkl} are one-body and two-body matrix elements that can be obtained from effective interaction theory, such as G-Matrix plus core polarization [19], which can be further refined using the experimental data [8, 20].

One can introduce the deformed single particle (s.p.) basis, which can be obtained from a constraint Hartree-Fock (HF) solution, or from the Nilsson s.p. Hamiltonian [18]. The deformed s.p. creation operator is given by the following transformation:

$$b_k^\dagger = \sum_i W_{ki} c_i^\dagger, \quad (2)$$

where the matrix elements $W_{ki} = \langle b_k | c_i \rangle$ are real in our calculation. The Slater Determinant (SD) built with the deformed single particle states is given by

$$|\kappa\rangle \equiv |s, \epsilon\rangle \equiv b_{i_1}^\dagger b_{i_2}^\dagger \dots b_{i_n}^\dagger | \rangle, \quad (3)$$

where s refers to the Nilsson configuration, indicating the pattern of the occupied orbits, and ϵ is the deformation

determined by the quadrupole ϵ_2 , hexadecupole ϵ_4 as in Ref. [18], but also octupole ϵ_4 , etc.

The general form of the nuclear wave function is taken as a linear combination of the projected SDs (PSDs),

$$|\Psi_{IM}^\sigma\rangle = \sum_{K\kappa} f_{IK\kappa}^\sigma P_{MK}^I |\kappa\rangle, \quad (4)$$

where \hat{P}_{MK}^I is the angular momentum projection operator. The energies and the wave functions [given in terms of the coefficients $f_{IK\kappa}^\sigma$ in Eq.(4)] are obtained by solving the following eigenvalue equation:

$$\sum_{K'\kappa'} (H_{K\kappa, K'\kappa'}^I - E_I^\sigma N_{K\kappa, K'\kappa'}^I) f_{IK\kappa'}^\sigma = 0, \quad (5)$$

where $H_{K\kappa, K'\kappa'}^I$ and $N_{K\kappa, K'\kappa'}^I$ are the matrix elements of the Hamiltonian and of the norm, respectively

$$H_{K\kappa, K'\kappa'}^I = \langle \kappa | H P_{K\kappa'}^I | \kappa' \rangle, \quad (6)$$

$$N_{K\kappa, K'\kappa'}^I = \langle \kappa | P_{K\kappa'}^I | \kappa' \rangle. \quad (7)$$

More details about the formalism can be found in Ref. [18].

III. CHOICE OF THE PCI BASIS

The analysis made in Ref. [18] indicated that one of the most important problems of the PCI method is a proper selection of the PCI basis. As introduced in our previous work [18], the general structure of the PCI basis is

$$\left\{ \begin{array}{l} 0p - 0h, \quad np - nh \\ |\kappa_1, 0\rangle, \quad |\kappa_1, j\rangle, \dots, \\ |\kappa_2, 0\rangle, \quad |\kappa_2, j\rangle, \dots, \\ \dots\dots\dots\dots\dots\dots\dots\dots\dots \\ |\kappa_N, 0\rangle, \quad |\kappa_N, j\rangle, \dots \end{array} \right\}. \quad (8)$$

where $|\kappa_i, 0\rangle$ ($i = 1, \dots, N$) is a set of starting states of different deformations. Assuming that we've found these $|\kappa, 0\rangle$ SDs (skipping the subscript i to keep notations short), relative *np-nh* SDs, $|\kappa, j\rangle$, on top of each $|\kappa, 0\rangle$ are selected using the constraint [18]

$$\Delta E = \frac{1}{2}(E_0 - E_j + \sqrt{(E_0 - E_j)^2 + 4|V|^2}) \geq E_{\text{cut}}, \quad (9)$$

where $E_0 = \langle \kappa, 0 | H | \kappa, 0 \rangle$, $E_j = \langle \kappa, j | H | \kappa, j \rangle$, $V = \langle \kappa, 0 | H | \kappa, j \rangle$ and E_{cut} is a parameter.

The $|\kappa, 0\rangle$ SDs need to be properly chosen in order to get good accuracy. In our previous work [18], we have chosen the SDs with the lowest unprojected expectation energy for each configuration, and we used the same basis for all the spins. That approach proved to work well for quite deformed nuclei, limiting its range of application. For instance, the description of ^{56}Ni with GXPF1A [20] exhibits a spherical ground state minimum which is selected as a basis SD. This spherical SD has a

good spin $I = 0$, which won't be useful if we calculate $I \neq 0$ states. This example suggests that a more efficient method may involve choosing different basis sets for different spins. Another problem with this method of selecting the $|\kappa, 0\rangle$ basis states is that for each configuration, only one SD was selected. Therefore some states, such as the β -vibrational states, cannot be described unless two or more shapes for the same configuration are artificially included outside of any algorithm.

To address these problems, we developed a new method of finding an efficient set of $|\kappa, 0\rangle$ states. The deformed single particle states are generated from the Nilsson Hamiltonian shown in Eq. (2) of Ref. [18]. For simplicity, we set

$$E_i = e_i. \quad (10)$$

In a first step, at each deformation $\epsilon = (\epsilon_2, \epsilon_3, \epsilon_4)$, we build many Slater determinants (SDs) denoted by $|s, \epsilon\rangle$, where s denotes a configuration of nucleons occupying the deformed single particle orbitals. These SDs are projected onto good angular momentum I , and the projected energy is calculated

$$E_{\text{exp}}(I, s, \epsilon) = \frac{\langle s, \epsilon | H P_{KK}^I | s, \epsilon \rangle}{\langle s, \epsilon | P_{KK}^I | s, \epsilon \rangle}. \quad (11)$$

We then identify the configuration s_a which has the lowest $E_{\text{exp}}(I, s, \epsilon)$ at each shape ϵ . Searching over all possible deformations ϵ , we obtain the energy surface of $E_{\text{exp}}(I, s_a, \epsilon)$ as a function of ϵ . The SD $|s_a, \epsilon_a\rangle$ which has the lowest $E_{\text{exp}}(I, s_a, \epsilon)$ is chosen as the first $|\kappa, 0\rangle$ state denoted as

$$|\kappa_1, 0\rangle = |s_a, \epsilon_a\rangle. \quad (12)$$

The next step is to find the second $|\kappa, 0\rangle$ state. We try all possible $|s, \epsilon\rangle$, and for each $|s, \epsilon\rangle$, we build the 2×2 Matrix pair (\mathbf{A}, \mathbf{B}) ,

$$\mathbf{A} = \begin{pmatrix} H_{11} & H_{12} \\ H_{21} & H_{22} \end{pmatrix}, \mathbf{B} = \begin{pmatrix} N_{11} & N_{12} \\ N_{21} & N_{22} \end{pmatrix},$$

where

$$H_{ij} = \langle i | H P_{MK}^I | j \rangle, N_{ij} = \langle i | P_{MK}^I | j \rangle, \quad (13)$$

$$\text{with } |i(j) = 1\rangle = |\kappa_1, 0\rangle, |i(j) = 2\rangle = |s, \epsilon\rangle. \quad (14)$$

Solving the generalized eigenvalue problem

$$\mathbf{A}x = \lambda \mathbf{B}x, \quad (15)$$

we get two eigenvalues, λ_1 and λ_2 , and their sum,

$$S_2 = \lambda_1^{(2)} + \lambda_2^{(2)}. \quad (16)$$

The SD $|s_b, \epsilon_b\rangle$ with the lowest S_2 is selected as the second $|\kappa, 0\rangle$ denoted as

$$|\kappa_2, 0\rangle = |s_b, \epsilon_b\rangle. \quad (17)$$

The process of finding more $|\kappa, 0\rangle$ SDs can be continued in a similar manner. Assuming that we have found the $(n-1)$ -th $|\kappa, 0\rangle$ SD, $|\kappa_{n-1}, 0\rangle$, then $|\kappa_n, 0\rangle$ is chosen as the $|s_x, \epsilon_x\rangle$, corresponding to the lowest S_n . Here,

$$S_n = \lambda_1^{(n)} + \lambda_2^{(n)} + \dots + \lambda_n^{(n)}. \quad (18)$$

and $\lambda_1^{(n)}, \lambda_2^{(n)}, \dots, \lambda_n^{(n)}$ are eigenvalues of Eq.(15) with

$$\mathbf{A} = \begin{pmatrix} H_{11} & H_{12} & \dots & H_{1n} \\ H_{21} & H_{22} & \dots & H_{2n} \\ \dots & \dots & \dots & \dots \\ H_{n1} & H_{n2} & \dots & H_{nn} \end{pmatrix}, \mathbf{B} = \begin{pmatrix} N_{11} & N_{12} & \dots & N_{1n} \\ N_{21} & N_{22} & \dots & N_{2n} \\ \dots & \dots & \dots & \dots \\ N_{n1} & N_{n2} & \dots & N_{nn} \end{pmatrix},$$

and

$$H_{ij} = \langle i | H P_{MK}^I | j \rangle, N_{ij} = \langle i | P_{MK}^I | j \rangle, \quad (19)$$

$$|i(j)\rangle = |\kappa_{i(j)}, 0\rangle, \text{ if } i(j) = 1, 2, \dots, n-1;$$

$$|i(j)\rangle = |s, \epsilon\rangle, \text{ if } i(j) = n. \quad (20)$$

Sometimes we may only use part of the S_n sum over the lowest λ_i 's as a selection criteria, i.e.,

$$S_n^k = \lambda_1^{(n)} + \lambda_2^{(n)} + \dots + \lambda_k^{(n)}, (1 \leq k \leq n), \quad (21)$$

and $S_n^n = S_n$ by definition.

Evaluating the projected energies for all SDs takes a long time to calculate, and not all of them may be necessary. Therefore, we enforce additional truncations. First, the HF energy, E_{HF} , is calculated. Next, at each shape ϵ , the SDs having all particles occupying the lowest Nilsson orbits are considered as the 0p-0h SDs. All particle-hole excitations up to 4p-4h built on these 0p-0h SDs are created, and their expectational energies

$$E_{\text{exp}}(s, \epsilon) = \langle s, \epsilon | H | s, \epsilon \rangle \quad (22)$$

are calculated. Those SDs satisfying $E_{\text{exp}}(s, \epsilon) - E_{\text{HF}} < E_{\text{expup}}$, where E_{expup} is a input parameter, are saved. Finally, the projected energies $E_{\text{exp}}(I, s, \epsilon)$ of the saved SDs are evaluated, and compared with the lowest projected energy $E_{\text{exp}}(I, s_a, \epsilon_a)$ available. We keep those SDs satisfying $E_{\text{exp}}(I, s, \epsilon) - E_{\text{exp}}(I, s_a, \epsilon_a) < E_{\text{pjup}}(I)$, where $E_{\text{pjup}}(I)$ is a input parameter, and we discard the others. The values of the parameters E_{expup} and $E_{\text{pjup}}(I)$ must be large enough so that the $|\kappa, 0\rangle$ can be properly chosen, but too large E_{expup} and $E_{\text{pjup}}(I)$ value may results in wasted computation without any improvement in accuracy.

Here we summarize the advantages of the new method of selecting the basis states $|\kappa, 0\rangle$. Firstly, as already mentioned, the method proposed in Ref. [18] uses the same $|\kappa, 0\rangle$ states for all spins, however, certain $|\kappa, 0\rangle$ states may not bring any contribution to certain spins. The new method improves the efficiency of the PCI basis, by choosing different $|\kappa, 0\rangle$ states for different spins.

Secondly, the $|\kappa, 0\rangle$ chosen by the new method may include two or more shapes for the same configuration s . Therefore, the present method explicitly includes the idea

imbedded in the Generator Coordinate Method (GCM) [21], and may be used to describe some collective vibrations, such as the β -vibration.

Thirdly, there are no limitations on the K values. In Ref. [18], we only selected basis states with relatively small- K values to keep the basis dimensions manageable. This limitation could be a problem in the case of the high spin states, for which the high- K configurations could be close to the yrast line. The new method described here selects basis states with all possible SDs satisfying $|K| \leq I$.

Finally, and perhaps more importantly, the drawback of getting large overlaps between different basis SDs, which is typical for an uncorrelated selections of the basis, is avoided by construction in the new method. Getting basis states with large overlaps leads to many spurious states due to the zero eigenmodes of the norm matrix. The significance of these zero modes is that some of the basis states that exhibit large overlaps bring insignificant contribution to the solutions of the Hill-Wheeler Eq. (5), while unnecessarily increasing the dimensions of the problem. Those useless SDs can be automatically filtered out by the present method because the overlap problem has been fully considered step-by-step when the generalized eigenvalue equations (15) are solved.

IV. CALCULATIONS OF ^{56}Ni

Using the new method, we recalculated the nuclei ^{56}Ni with GXPF1A interaction[20]. Let's first consider the case of $I = 0$. Both ϵ_2 and ϵ_4 span the interval from -0.45 to 0.45 in steps of 0.03 . The first basis state, $|\kappa_1, 0\rangle$, having the lowest projected energy, corresponds to $I = 0$. In Fig. 1, the surfaces of the $E_{\text{exp}}(I, s_a, \epsilon)$ (See Eq. (11)) and $E_{\text{exp}}(s_a, \epsilon)$ (See Eq. (22)) are plotted as functions of ϵ_2 and ϵ_4 . Our calculation shows that the configuration s_a has all 16 valence particles in ^{56}Ni occupying the orbits coming from the $1f_{7/2}$ subshell. The unprojected minimum, Fig. (1)(a) is at -203.800 MeV, and its shape is spherical, consistent with the HF result. However, the projected energy surface presents a quite different picture. There are four minima around the spherical shape, the lowest one has -204.473 MeV and a small oblate deformation, $\epsilon_2 = -0.09$ and $\epsilon_4 = -0.09$. This energy is 673 keV lower than the HF energy, and 1.236 MeV above the exact CI ground state energy of -205.709 MeV. This $|\kappa, 0\rangle$ state is a good candidate for the ground state.

The second basis state, $|\kappa_2, 0\rangle$, has the same configuration as the first one, but a different shape characterized by $\epsilon_2 = -0.24$ and $\epsilon_4 = -0.15$. Comparing with Fig. 1, this shape is quite different from any of the remaining 3 minima. The reason is that the SDs at those 4 minima are highly overlapping each other after the angular momentum projection. Once the lowest one is picked up, the others will automatically be filtered out by the present method. The $|\kappa_2, 0\rangle$ corresponds to the first excited 0^+ state, which might be called a β -vibrational state.

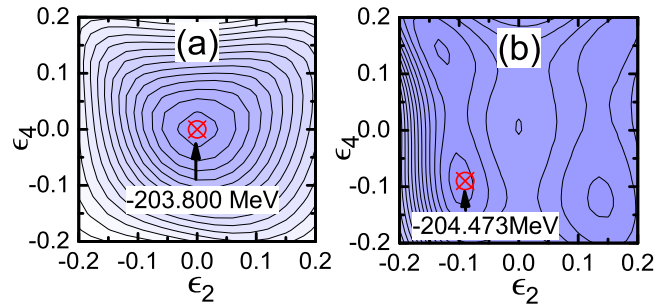


FIG. 1: (Color online) Unprojected energy surface (left panel) and the projected energy surface with $I = 0$ (right panel) for the ground state of ^{56}Ni with the GXPF1A interaction. The lowest energy is marked by ' \oplus '

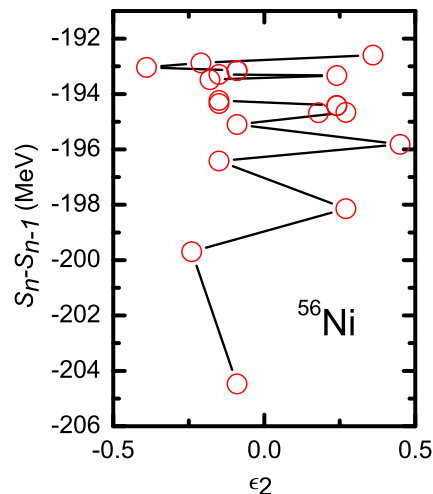


FIG. 2: (Color online) $S_i - S_{i-1}$ values of $|\kappa_i, 0\rangle$ at $I = 0$ for ^{56}Ni as a function of ϵ_2 . ϵ_4 are included in the calculation. $|\kappa_1, 0\rangle$ is the lowest one.

The third basis state, $|\kappa_3, 0\rangle$, has a prolate shape with $\epsilon_2 = 0.27$ and $\epsilon_4 = 0.06$. Its configuration can be obtained starting from $|\kappa_1, 0\rangle$, but with 4 particles jumping from the $|\Omega| = 7/2$ ($1f_{7/2}$) orbits to the $|\Omega| = 1/2$ ($2p_{3/2}$) orbits. $|\kappa_3, 0\rangle$ can generate a deformed rotational band, which has been observed in experiments [22]. Here, we only create the band head, which is the third 0^+ state. Informations about higher $|\kappa, 0\rangle$ SDs are shown in Fig. 2. The value $S_i - S_{i-1}$ indicates the energy position of each $|\kappa_i, 0\rangle$ state.

Once we have selected the $|\kappa, 0\rangle$ SDs, we perform the PCI calculations. There are two parameters used in PCI: one is the number of $|\kappa, 0\rangle$ SDs, n , and the other is the E_{cut} used in Eq. (9) to select the number of particle-hole excitations on top of each $|\kappa, 0\rangle$ [18].

It is interesting to study how many $|\kappa, 0\rangle$ are needed to describe the low-lying states. Fig. (3)(a) shows the

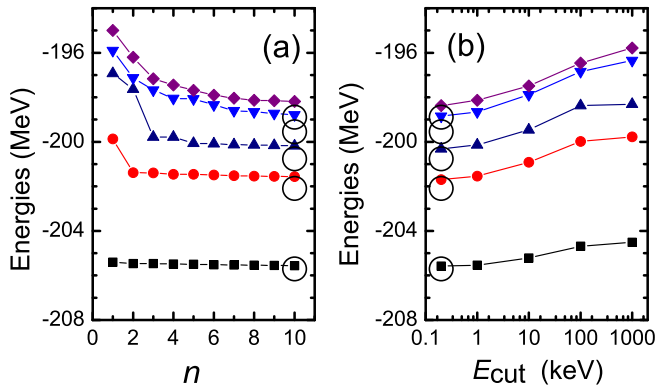


FIG. 3: (Color online) Left panel, $I = 0$ PCI energies for ^{56}Ni as functions of n with $E_{\text{cut}} = 1$ keV. Right panel, $I = 0$ PCI energies for ^{56}Ni as functions of $E_{\text{cut}} = 1$ with $n = 8$. Full CI results are also shown as the open circles by comparison.

PCI energies as functions of n for $E_{\text{cut}} = 1$ keV. For $n = 1$ the PCI dimension is only 180, yet the first 0^+ PCI energy is -205.409 MeV, only 300 keV above the exact full CI value. $|\kappa_2, 0\rangle$ must be included to describe the second 0^+ state, and $|\kappa_3, 0\rangle$ reproduces the third 0^+ state. To accurately describe more excited states more $|\kappa, 0\rangle$ SDs are needed. For the lowest 5 states in ^{56}Ni a good approximation can be achieved starting with $n = 7$. If one keeps on increasing n , then those 5 energies will become closer and closer to the CI values. For instance, with $n = 15$, the the ground state PCI energy becomes -205.603 MeV, just 100 keV above the exact value.

The PCI energies are also affected by the E_{cut} parameter. For $E_{\text{cut}} = 1000$ keV no particle-hole excited SDs are included, and the PCI dimension is the same as the number of $|\kappa, 0\rangle$ SDs included, $n = 8$ in this case. Therefore the PCI energies are exactly the values of λ_i in Eq. (18). More particle-hole excited SDs can be included by reducing the value of E_{cut} . For example, by decreasing from $E_{\text{cut}} = 1000$ keV to $E_{\text{cut}} = 1$ keV, the PCI energies drop $\sim 1.0 \div 2.3$ MeV for the lowest 5 states, and become close to the full CI values. By decreasing from $E_{\text{cut}} = 1$ keV to $E_{\text{cut}} = 0.2$ keV the energy drop becomes slower, and is around $\sim 100 \div 200$ keV. The PCI energies for $I \neq 0$ states are also calculated, and shown in Fig. 4, the number of $|\kappa, 0\rangle$ is $n = 15$ and $E_{\text{cut}} = 1$ keV. One can observe good agreements between the PCI and the CI results, including the states in the rotational band starting at about 5 MeV.

V. CALCULATIONS IN $f5pg9$ VALENCE SPACE

We have also extended our calculations to the $f5pg9$ valence space, which includes the $1f_{5/2}$, $2p_{3/2}$, $2p_{1/2}$, and the $1g_{9/2}$ spherical shells. $1g_{9/2}$ orbital has positive parity, and the other fp orbitals have negative parity. Therefore, SDs with both parities can be built for any num-

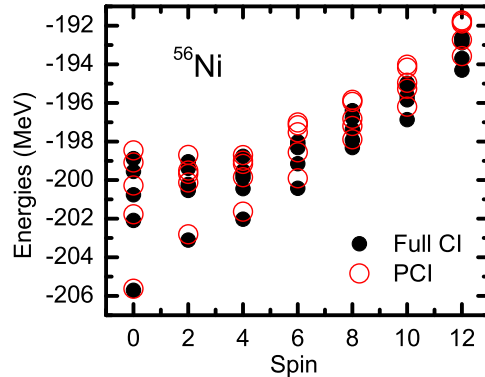


FIG. 4: (Color online) The lowest 5 energies at each spin for ^{56}Ni calculated using PCI (open circles) and full CI (filled circles).

ber of nucleons. The positive parity SDs are those with even number particles occupying the fp orbitals, while the negative parity SDs have odd number particles occupy the fp orbitals. The angular momentum projection does not change the parity. The parity of the projected states remain the same as that of the original SDs. Therefore, one can split the PCI basis into the positive parity part, I^+ , and the negative parity part, I^- , at each spin I . With the present method, different $|\kappa, 0\rangle$ SDs can be generated separately for the I^+ basis and I^- basis.

The interaction for $f5pg9$ shell space was taken from Ref. [23]. It includes, besides the usual quadrupole, hexadecupole, and pairing terms, octupole contributions and monopole corrections. In all cases, 20 $|\kappa, 0\rangle$ SDs are taken for each I^π basis and E_{cut} was fixed to 1 keV. The first example we analyze is the $N=Z$ nucleus ^{68}Se , which is known to be deformed with competing oblate and prolate deformations. The energies of the 20 $|\kappa, 0\rangle$ SDs for both $I^\pi = 0^+$ basis and $I^\pi = 0^-$ basis are shown in Fig. 5.

It is known that ^{68}Se nucleus exhibits shape coexistence features. The constrained HF calculations of Ref. [23] as well as our results in Fig. 6 show that there are two minima. Both of them are axially and reflection symmetric. The lowest minimum has -40.718 MeV and oblate shape, and the second one has -39.956 MeV and prolate shape. It is interesting that the results of our new method presents the same picture as one can observe in the left panel of Fig. 5, where the lowest $|\kappa_1, 0\rangle$ is oblate with $S_1 = E_{\text{exp}}(0, s_a, \epsilon_a) = -42.405$ MeV and $|\kappa_2, 0\rangle$ is prolate with $S_2 - S_1 = -41.549$ MeV. However, both energies are about 1.6 MeV lower than those obtained by an HF procedure, due to the angular momentum projection.

For the 0^- basis the lowest $|\kappa, 0\rangle$ SD lies at -36.44 MeV, which is relatively high (see Fig.5), and has a prolate shape. The corresponding configuration is the same as that of the second HF minimum, except that

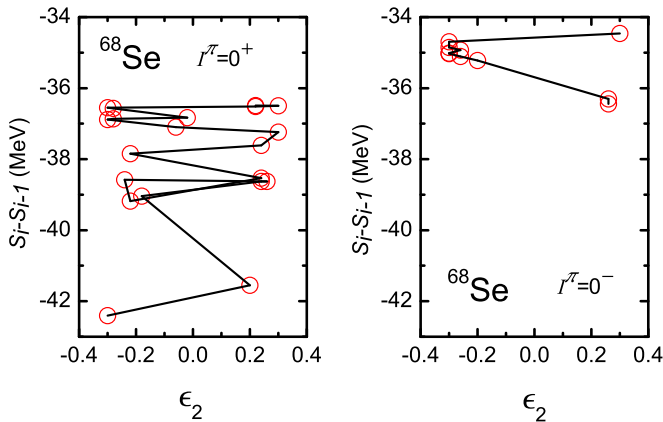


FIG. 5: (Color online) $S_i - S_{i-1}$ values of $|\kappa_i, 0\rangle$ for $I^\pi = 0^+$ (left) and $I^\pi = 0^-$ (right) in ^{68}Se as a function of ϵ_2 . ϵ_4 are included in the calculation.

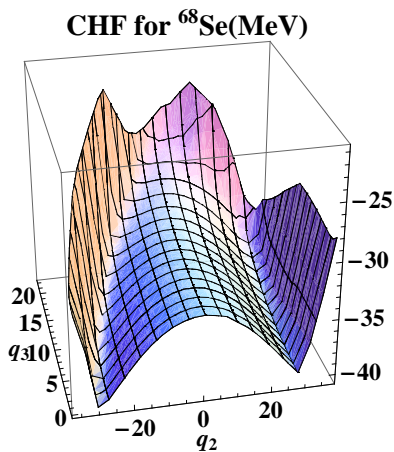


FIG. 6: (Color online) Energy surface provided by Constrained Hartree-Fock (CHF) calculations as a function of $q_2 = \sqrt{\frac{16\pi}{5}} \left(\frac{r}{b}\right)^2 Y_{20}$ and $q_3 = \left(\frac{r}{b}\right)^3 Y_{30}$. (b is the harmonic oscillator length)

one particle was excited from the $\Omega = 3/2(p_{3/2})$ orbital to the $\Omega = 3/2(g_{9/2})$ orbital. Because ^{68}Se has $N = Z$, this excited particle can be either a neutron or a proton, and therefore there are two different $|\kappa, 0\rangle$ SDs with the same shape and the same low energy. Similar cases appear for other $|\kappa, 0\rangle$ SDs. Therefore, in Fig. 5(b) each symbol corresponds to two different $|\kappa, 0\rangle$ SDs. The position of the second lowest symbol is only about 130 keV above the lowest one, and its configuration is similar to the lowest one, but with the odd particle excited from the $\Omega = 1/2(p_{3/2})$ orbital to the $\Omega = 1/2(g_{9/2})$ orbital.

Using the $|\kappa, 0\rangle$ states described in Fig. 5, one can calculate the PCI energies for the 0^+ and 0^- states, which turned out to be very close to the CI results. For $I \neq 0$, similar good results have also been achieved, as shown in Fig. 7.

As indicated in the above discussions, the PCI method

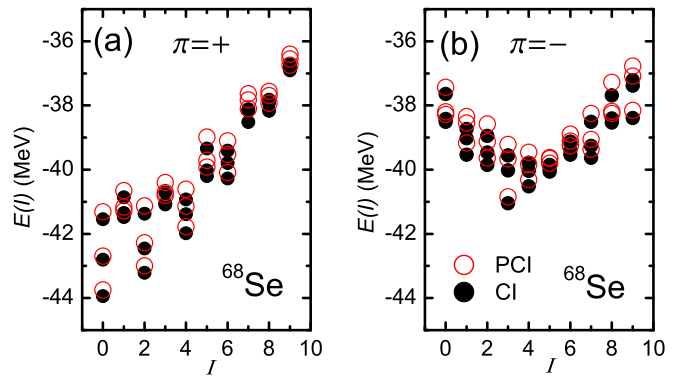


FIG. 7: (Color online) The lowest 3 energies at each spin/parity for ^{68}Se calculated using PCI (open circles) and full CI (filled circles).

TABLE I: PCI Dimensions compared with those of full CI for ^{70}Se

| Spin (I) | $\pi = +$ | | $\pi = -$ | |
|-----------------|-----------|-------------------|-----------|-------------------|
| | PCI | CI | PCI | CI |
| 0 | 3665 | 6.7×10^6 | 4497 | 6.7×10^6 |
| 1 | 4735 | 2.0×10^7 | 4431 | 2.0×10^7 |
| 2 | 4369 | 3.2×10^7 | 4284 | 3.2×10^7 |
| 3 | 4799 | 4.2×10^7 | 4778 | 4.2×10^7 |
| 4 | 4384 | 5.0×10^7 | 4476 | 5.0×10^7 |
| 5 | 4714 | 5.5×10^7 | 4284 | 5.5×10^7 |
| 6 | 4246 | 5.8×10^7 | 4636 | 5.8×10^7 |
| 7 | 4505 | 5.9×10^7 | 4159 | 5.9×10^7 |
| 8 | 4125 | 5.7×10^7 | 4056 | 5.7×10^7 |

not only provides a good approximation for the CI results, but it is also a convenient tool to gain some insight into the physics of the nuclear states. One interesting example is the lowest state in Fig. 7(b), which is a 3^- state. As shown in Fig. 8, the (lowest) $|\kappa_1, 0\rangle$ SD has $K^\pi = 3^-$ and oblate deformation. The configuration of this $|\kappa_1, 0\rangle$ is the same as the oblate HF minimum, except that one particle was excited from the $\Omega = 3/2(p_{3/2})$ orbital to the $\Omega = 9/2(g_{9/2})$ orbital to form a $K^\pi = 3^-$ SD. The second SD, $|\kappa_2, 0\rangle$, has the same energy and the same shape as $|\kappa_1, 0\rangle$ because $N = Z$, and due to the isospin symmetry of the adopted Hamiltonian. If only the particle-hole excitations built on $|\kappa_1, 0\rangle$ are included, one obtains a PCI energy of -40.469 MeV. If the $|\kappa_2, 0\rangle$ SD is further included, the PCI energy drops 300 keV to -40.769 MeV. This energy is only 300 keV above the exact value of -41.043 MeV. However, the PCI energy for $n = 20$ is -40.843 MeV, only 70 keV lower than what one can obtain with $n = 2$. Therefore, it is clear that the lowest 3^- state has mostly contributions from the lowest 2 oblate $K^\pi = 3^-$ SDs, i.e. $|\kappa_1, 0\rangle$ and $|\kappa_2, 0\rangle$.

We have also calculated states of both parities in ^{70}Se . The results are shown in Fig. 9. Once again, the PCI

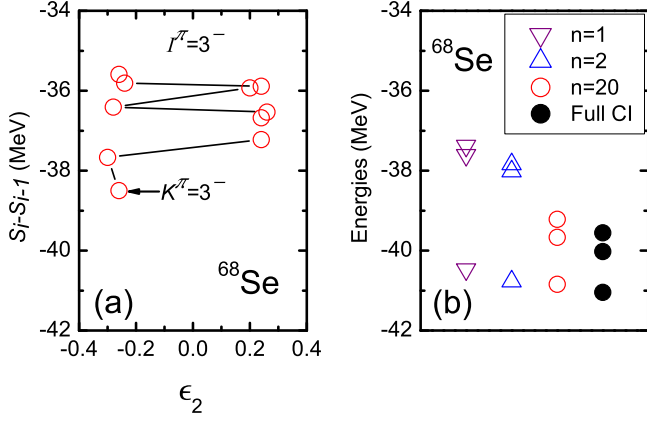


FIG. 8: (Color online) (a), $S_i - S_{i-1}$ values of $|\kappa, 0\rangle$ at $I^\pi = 3^-$ in ^{68}Se . (b), PCI energies (Open Symbols) and CI energies (Fill Circles) at $I^\pi = 3^-$ in ^{68}Se . The open Symbols from left to right refer to PCI calculations with $n = 1, 2$ and 20 .

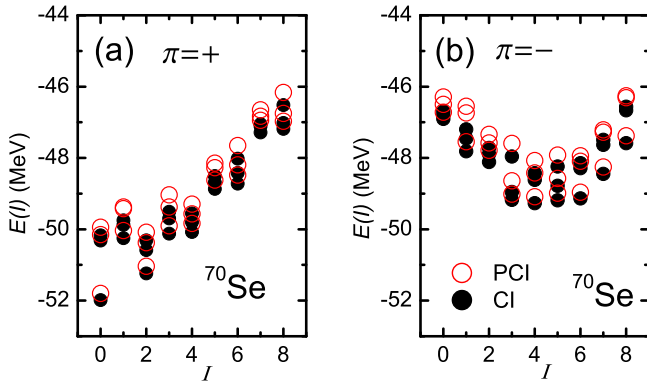


FIG. 9: (Color online) The same as Fig. 7 but for ^{70}Se .

results are very close to those of full CI for both positive parity and negative parity for a wide range of spin values. However, much smaller dimensions of the PCI matrices are necessary. The PCI dimensions corresponding to the I^π calculations in Fig. 9 are compared in Table I with the full coupled-I CI dimensions. The PCI dimensions are small fractions, roughly 10^{-4} , of the full CI dimensions. As is well known, the most serious problem with full CI method is the explosion of the dimensions as the number of the single-particle valence states, and/or number of valence nucleons. However, this problem seems to be less of an issue for the PCI method. The total PCI dimension can be estimated as the product of two numbers, $n \times m$, where n is the number of $|\kappa, 0\rangle$ states and m is the number of particle-hole excitations selected by E_{cut} in Eq. (9). Our investigations indicate that n is related to how many low-lying states of a given spin one wants to accurately describe. For instance, if we are interested in only the yrast state, quite often a good approximations can be obtained with $n = 1$ or 2 . $n = 20$ seems to be enough to describe the lowest 3-5 states of each I^π in the present

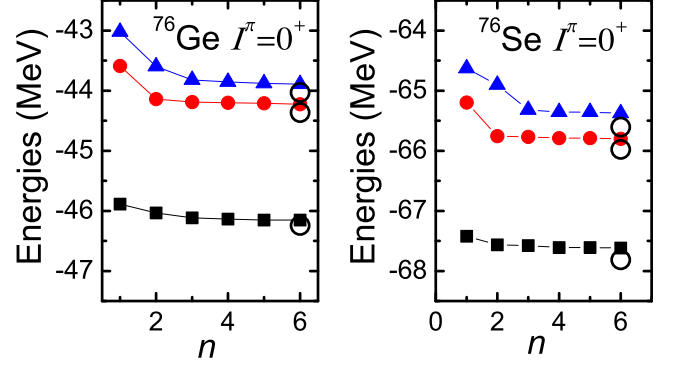


FIG. 10: (Color online) Lowest 3 0^+ energies of ^{76}Ge and ^{76}Se calculated by PCI (filled symbols) and full CI (open circles)

calculations. As regarding m , the $|\kappa, j\rangle$ SDs are limited to 1p-1h and 2p-2h excitations according to Eq. (9). Note that $|\kappa, j\rangle$ has the same K^π as that of $|\kappa, 0\rangle$. As the parameter E_{cut} is enforced via Eq. (9), m can be significantly reduced. For instance, in the case of $I^\pi = 0^+$ for ^{70}Se , $m_{2p2h} = 801$ for $|\kappa_1, 0\rangle$, but only 138 SDs were finally included if $E_{\text{cut}} = 1$ keV.

The exploding CI dimensions has as a consequence a rapid increase of the computing time necessary for full CI calculation. Using the modern coupled-I code NuShellX [4], the full CI calculation of all states in Fig. 9 could take almost one year when only one processor is used. The calculation of the lowest 3 states of each I^π in ^{70}Se would take in average about 20 days. For the same calculation, PCI takes around 5 hours for each I^π . The main computational workload in PCI is related to the calculation of the dense matrices H , and N in Eq. (6). It should be metioned that extra time is needed to search for the optimized set of $|\kappa, 0\rangle$ SDs. The computing time can be affected by: (1) the number of mesh points used for the shape paramters; (2) the values of the parameters E_{expup} and $E_{\text{pjup}}(I^\pi)$ that decides how many SDs are considered in the optimization process; (3) the total number n of $|\kappa, 0\rangle$ basis states selected; (4) the value of E_{cut} . For example, in the calculation of $I^\pi = 0^+$ in ^{70}Se , both ϵ_2 and ϵ_4 run from -0.3 to 0.3 in steps of 0.02 , $E_{\text{expup}} = 7$ MeV and $E_{\text{pjup}}(I^\pi = 0^+) = 5$ MeV, and $E_{\text{cut}} = 1$. Under these conditions, it will takes about 10 hours to obtain 20 $|\kappa, 0\rangle$ SDs using one processor. For other I^π , the computational time ranges from few hours to 1 or 2 days. However, the total time for a PCI calculations is at least 10 times shorter than that of the corresponding full CI calculation for the case of ^{70}Se .

Finally, we used the new PCI method to calculate the low lying 0^+ states in ^{76}Ge and ^{76}Se . The nuclear structure of these two nuclei is relevant for the double beta decay (DBD) process of ^{76}Ge . DBD is one of the most actively investigated nuclear physics problem, which may reveal new physics beyond the Standard Model, including the absolute values of the neutrino masses. Full CI

calculations [24, 25, 26] of the 2-neutrino and neutrinoless DBD matrix elements have been carried out for some DBD nuclei up to ^{136}Xe . However, for heavier DBD nuclei ^{150}Nd and ^{238}U , the huge CI dimensions make the full CI calculation unmanageable. PCI can take full advantage of the deformation, and an efficient truncation could be obtained for well deformed nuclei, such as ^{150}Nd and ^{238}U . As a first inroad into this problem, the low-lying 0^+ states ^{76}Ge and ^{76}Se are calculated using the present version of the PCI, and are compared with full CI results in Fig. 10. Using only 6 $|\kappa, 0\rangle$ SDs ($n = 6$) for each nucleus, the PCI dimensions are 561 and 647 for ^{76}Ge and ^{76}Se , respectively. The calculated PCI energy of the lowest 0^+ state for ^{76}Se is 200 keV higher than the exact value, and only 86 keV higher for ^{76}Ge . In addition, good approximations for the excited 0^+ states have also been reached. Given these encouraging results, one would hope that PCI calculations could be successfully performed for the heavy deformed DBD nuclei, such as ^{150}Nd and ^{238}U , in a not so distant future.

VI. CONCLUSIONS AND OUTLOOK

In this article we propose a newly improved algorithm of selecting the basis of Slater determinants that can be used with the Projected Configuration Interaction method introduced in Ref. [18]. The new algorithm depends on a number of parameters that can be used to fine tune its efficiency. Its main advantages over the original method of selecting of the basis are summarized at the end of Section III.

We used the new algorithm to revisit the calculation of ^{56}Ni , quasi-spherical nucleus that has a relatively low-

lying rotational band. We were able to calculate its low-lying states very efficiently, and with good accuracy, gaining also insight into the physics of these states. We have also use the new method to analyze some Se and Ge isotopes in the $f5pg9$ valence space. Both natural and unnatural parities can be accurately described for these nuclei, even for cases with pronounced competing deformations, such as ^{70}Se and ^{70}Ge . The PCI dimensions are significantly lower the corresponding CI dimensions, as well as the corresponding computational effort. In addition, in most cases, the low-lying projected basis states can provide some physical insight into the structure of the low-lying states. Finally, we calculated with the new method the low-lying 0^+ states in ^{76}Ge and ^{76}Se that are relevant for the double beta decay of ^{76}Ge . The hope is that this method could be used some day to study the double beta decay of the strongly deformed ^{150}Nd and ^{238}U .

Further improvements to the PCI method will include the extension of the formalism developed in Ref. [18] to calculate electromagnetic transition probabilities. The new method uses different bases for different spins, which introduces additional complications. Other observables, such as spectroscopic amplitudes and DBD matrix elements have to be worked out. Further improvement of the basis may be achieved for some cases that exhibit significant octupole deformation, which will require full projection on good parity.

Acknowledgments

The authors acknowledge support from the DOE Grant No. DE-FC02-09ER41584. M.H. acknowledges support from NSF Grant No. PHY-0758099. Z.G. acknowledges the NSF of China Contract Nos. 10775182, 10435010 and 10475115.

-
- [1] B.A. Brown and B.H. Wildenthal, *Ann. Rev. Nucl. Part. Sci.* **38**, 29 (1988).
 - [2] E. Caurier, Martinez-Pinedo, F. Nowacki, A. Poves, and A. P. Zuker, *Rev. Mod. Phys.* **77**, 427 (2005).
 - [3] E. Caurier and F. Nowacki, *Acta Physica Polonica* **30**, 705 (1999).
 - [4] W.D.M. Rae, NuShellX code 2008, <http://knollhouse.org/NuShellX.aspx>
 - [5] B. H. Wildenthal, *Prog. Part. Nucl. Phys.* **11**, 5 (1984).
 - [6] A. Poves, and A. P. Zuker, 1981a, *Phys. Rep.* **71**, 141.
 - [7] W. A. Richter, M. J. van der Merwe, R. E. Julies, and B. A. Brown, 1991, *Nucl. Phys. A* **523**, 325.
 - [8] M. Honma, T. Otsuka, B. A. Brown, and T. Mizusaki, *Phys. Rev. C* **65**, 061301(R)(2002).
 - [9] K. Hara and Y. Sun, *Int. J. Mod. Phys. E* **4**, 637(1995).
 - [10] Y. S. Chen and Z. C. Gao, *Phys. Rev. C* **63** 014314(2000).
 - [11] S. Mishra, A. Suhkla, and V.K.B. Kota, *Phys. Rev. C* **78**, 024307 (2008).
 - [12] S. G. Nilsson. *Dan. Mat. Fys. Medd* **29** nr.16(1955)
 - [13] J. P. Elliott, *Proc. R. Soc. London, Ser. A* **245**, 128,562(1958).
 - [14] J.A. Sheikh and K. Hara, *Phys. Rev. Lett.* **82**, 3968(1999).
 - [15] Z. C. Gao, Y. S. Chen, and Y. Sun, *Phys. Lett.* **B634** 195(2006).
 - [16] K.W. Schmid, *Prog. Part. Nucl. Phys.* **52**, 565(2004)
 - [17] M. Honma, T. Mizusaki, and T. Otsuka, *Phys. Rev. Lett.* **77**, 3315 (1996).
 - [18] Z.-C. Gao and M. Horoi, *Phys. Rev. C* **79**, 014311 (2009).
 - [19] M. Hjorth-Jensen, T. T. S. Kuo and E. Osnes, *Phys. Rep.* **261**, 125 (1995).
 - [20] M. Horoi, B. A. Brown, T. Otsuka, M. Honma, and T. Mizusaki, *Phys. Rev. C* **73** 061305(R)(2006).
 - [21] D. L. Hill and J. A. Wheeler, 1953, *Phys. Rev.* **89**, 1102.
 - [22] D. Rudolph et al., *Phys. Rev. Lett.* **82**, 3763 (1999).
 - [23] K. Kaneko, M. Hasegawa, and T. Mizusaki, *Phys. Rev. C* **70**, 051301(R) (2004).
 - [24] E. Caurier, F. Nowacki, A. Poves, and J. Retamosa, *Phys. Rev. Lett.* **77**, 1954 (1996).
 - [25] M. Horoi, S. Stoica, and B.A. Brown, *Phys. Rev. C* **75**, 034303 (2007).
 - [26] E. Caurier, J. Meneñdez, F. Nowacki, and A. Poves, *Phys. Rev. Lett.* **100**, 052503 (2009).